Pergamon
www.elsevier.com/locate/asr

Adv. Space Res. Vol. 30, No. 12, pp. 2809–2814, 2002

Printed in Great Britain
0273-1177/02 $22.00 + 0.00

PII: S0273-1177(02)00763-9

ANALYSIS OF THE TURBULENCE OBSERVED IN THE OUTER CUSP TURBULENT BOUNDARY LAYER

J. S. Pickett[1], J. D. Menietti[1], G. B. Hospodarsky[1], D. A. Gurnett[1], and K. Stasiewicz[2]

[1] *Department of Physics and Astronomy, The University of Iowa, Iowa City, IA 52242, USA*
[2] *Swedish Institute of Space Physics, Uppsala, Sweden*

ABSTRACT

One of the prominent features of the cusp Turbulent Boundary Layer (TBL) is a persistent low frequency electromagnetic turbulence that extends from <1Hz up to the electron cyclotron frequency, accompanied by what appears to be purely electrostatic noise above this frequency range. The Plasma Wave Instrument onboard Polar obtained plasma wave measurements in the cusp TBL in the form of waveform captures simultaneously from 6 different sensors (3 each orthogonal electric and magnetic) in the frequency range 1 Hz up to 25 kHz. This allowed us to directly calculate the phase velocity from the measured ratio of |dE| to |dB| and compare it to theoretical values for various modes. Using this technique, we have gained some insight into the mode of the electromagnetic turbulence that extends in frequency from ~1 Hz up to the electron cyclotron frequency (several hundred Hz to a few kHz) in the TBL. The whistler and kinetic Alfvén wave modes are discussed as the possible modes of this turbulence. By analyzing the high time resolution waveforms, we isolate and identify some of these modes. The electrostatic turbulence above the electron cyclotron frequency is associated with pulses and quasi-sinusoidal waveforms observed in the measured time series. These do not fit any known mode, although work is continuing in this area to show that some of them may be associated with electron holes or with downshifted Langmuir waves produced through a two-stream instability.

INTRODUCTION

The Turbulent Boundary Layer (TBL) has been distinguished by Savin et al. (1998) as a distinct region just outside and/or at the near-cusp magnetopause and is best characterized by extreme magnetic turbulence and magnetic field vortices. The orbit of the Polar spacecraft is ideal for investigating the various characteristics of the cusp TBL at 7-9 R_E. The wave environment in the cusp TBL is quite complex as shown by the wave observations from the Polar spacecraft that were presented in Pickett et al. (2000, 1999a,b). Typically, broadband magnetic turbulence is observed in the TBL from the lowest frequencies measured (~1 Hz), which is below the lower hybrid resonance frequency, up to the electron cyclotron frequency (f_{ce}), typically several hundreds of Hz to a few kHz. In addition, coherent sinusoidal waveforms are often found imbedded in the electromagnetic turbulence at frequencies of around a few tens of Hz, few hundreds of Hz, and just below f_{ce} (Pickett et al., 2000). Above f_{ce} is a broad band of electrostatic noise associated with pulses and quasi-sinusoidal waveforms in the time domain (Pickett et al., 2000). The purpose of this paper is to further the work begun in those earlier studies of the waves in the cusp TBL by comparing the measured value of the ratio of the wave electric field to wave magnetic field (phase velocity) using the Polar measurements, to the theoretical value of the same ratio obtained from the dispersion relation in order to determine what modes are present.

Data from the Polar Plasma Wave Instrument (PWI) (Gurnett et al., 1995) waveform receivers are used in this study. These data provide three simultaneous, orthogonal, high time resolution components of each of the electric and magnetic field waveforms in snapshot form, i.e., the data are sampled every few seconds or minutes, rather than continuously. Thus, unlike similar studies in the past, we can obtain the amplitudes of the wave electric and magnetic fields directly without having to resort to making assumptions about magnitude and direction of a second or third component. We can then eliminate this as a possible source of error when comparing measured and theoretical values.

OBSERVATIONS AND COMPARISON TO THEORY

A typical set of waveforms obtained in the cusp TBL at 8 R_E, 13.2 MLT (Magnetic Local Time), and 51.5° λ_m (magnetic latitude) are shown in Figure 1a. Plotted in this figure are the calibrated waveforms obtained in the frequency range of 1-25 Hz over a period of 4.64 s. The top three panels are the three orthogonal components of the time derivative of the electric field, in mV/m, and the bottom three panels are the three orthogonal components of the time derivative of the magnetic field, in nT/sec, all presented in a local magnetic field-aligned coordinate system. In this system, the Z-component lies in the direction of the local DC magnetic field (parallel to **B**) as measured by Polar MFE, the X-component is chosen so that the radial vector outward from the center of the earth to the spacecraft location, **R**, is in the meridian plane (contained in the north-south, or X-Z plane, and perpendicular to **B**), and the Y-component completes the right-handed coordinate system, being generally eastward (perpendicular to **B**). The magnetic field components are presented in nT/sec rather than the usual nT because the response of the magnetic search coil antennas is not flat across the entire bandpass of the receiver. Most of the resolution of the higher frequency components would be lost in the time series if the data were calibrated in nT. The important thing to note in Figure 1a is that turbulence is observed in both the electric and magnetic components throughout the entire plot, and that there appears to be some correlation between the two.

Figure 1b contains the transformation of the wave data from Figure 1a into the frequency domain. Plotted in this figure is the measured phase velocity (light solid line) obtained from transforming the three components of each of the wave electric and magnetic fields into the frequency domain and computing the ratio of |dE| to |dB| to get phase velocity, in km/sec. The solid bold line in Figure 1b is the value of |dE|/|dB| for the noise computed from flight data by averaging in the frequency domain the electric and magnetic field components which were obtained from a continuous time interval of a few hours length during quiet magnetospheric conditions. This procedure was performed separately for all of PWI's receivers and for all of the different filter modes of each receiver since the filter characteristics can vary significantly from one digital filter to another depending on how it was designed. This value of |dE|/|dB| for the noise is extremely valuable because it allows us to determine where, in frequency, a real emission is probably being recorded by its deviation from the noise curve. Depending on whether the data deviate above (or below) the noise curve determines whether the emission is more electrostatic (or more electromagnetic). In Figure 1b we note that there appears to be a real emission that is more electrostatic from 1 Hz to about 8 Hz because of its deviation above the noise curve at these frequencies.

We now compare the measured emission to the theoretical value of the dispersion relation for Kinetic Alfvén Waves (KAW) as derived by Stasiewicz et al. (2000b), which should be observed on a spacecraft as a frequency

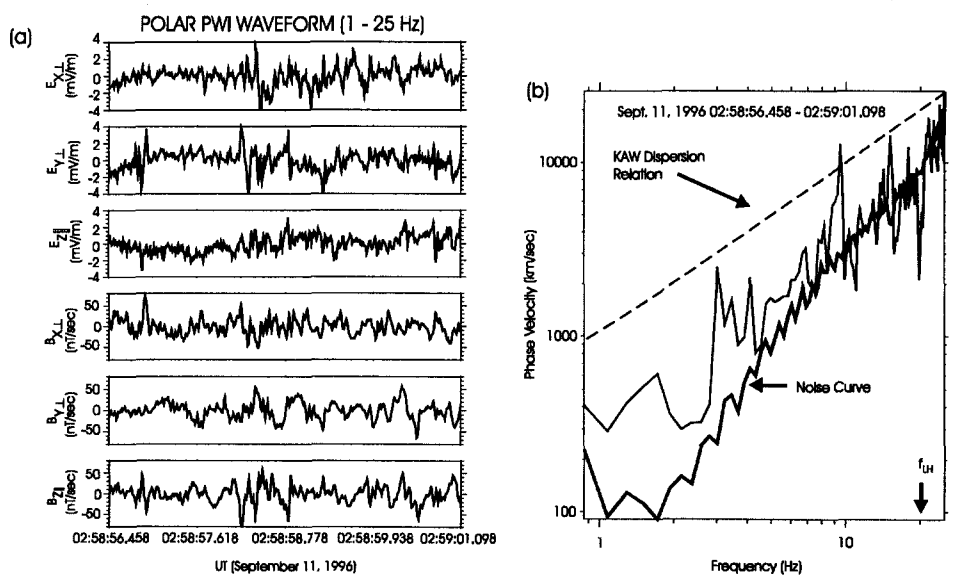

Fig. 1. (a) Recorded time series covering 4.64 s from six channels of the Polar Plasma Wave Instrument transformed to a local magnetic field-aligned coordinate system. (b) Measured phase velocity (light solid line) obtained from the data plotted in (a), noise curve (solid dark line) determined from in-flight data with fluctuations above and below the noise curve indicating possible real emissions, and theoretical dispersion curve for Kinetic Alfvén Waves (dashed line).

spectrum, $|\delta E/\delta B| \approx v_A [1 + (2\pi f(\rho_i/v))^2]^{1/2}$, where v_A is the Alfvén velocity computed from $v_A \approx (2.2x10^{11}B_o)/n^{1/2}$ in cm/sec with n the plasma density in cm^{-3} and B_o the measured magnetic field in nT; f is the measured frequency in Hz; ρ_i is the ion thermal gyroradius = $(T_e/m_i)^{1/2}/\omega_{ci}$ determined from Polar Hydra and MFE data with T_e the electron temperature, m_i the mass of the ions and ω_{ci} the ion cyclotron frequency; and v is the velocity of the plasma structure $\approx v_E$ (convective velocity) $\approx$ 100 km/s for the time period shown in Figure 1 based on measured E and B fields by Polar EFI and MFE, respectively. The convective speed is used since the satellite velocity (~3 km/sec) is much smaller than the convective flow. A similar dispersion relation was developed to compare to Freja data (Stasiewicz et al., 2000a). However, for Freja the dispersion relation was developed for Inertial Alfvén Waves (IAW). The differences in the IAW and KAW relations are that the collisionless electron skin depth is used for IAW rather than ion gyroradius as for KAW, and the Freja spacecraft velocity was used for IAW instead of convective flow for KAW. During the time of the data shown in Figure 1, B_o = 31.3 nT, ρ_i = 81.5 km, n = 10 cm^{-3}, and the ion species was assumed to be hydrogen. The KAW dispersion relation is plotted as a dashed line in Figure 1b. The emission from 1 Hz to 8 Hz does not fit on this theoretical curve, but it does show a trend toward it. This may imply that the low frequency turbulence is composed of more than one mode. Since there appears to be some correlation between the measured electric and magnetic components as seen in the time domain, it is likely that some of the turbulence represents spatial (Δk), rather than temporal ($\Delta\omega$), turbulence of kinetic Alfvén waves that are Doppler-shifted to higher frequencies by convective plasma flows (Stasiewicz et al., 2000a,b) as discussed above. In addition, it is possible that some of the turbulence is created through the lower hybrid drift instability since the turbulence occurs just below the lower hybrid frequency.

Moving to higher frequencies, we have plotted in Figure 2a the 6 components of the electric and magnetic field waveforms covering ~57 ms in the magnetic field-aligned coordinate system described above. These waveforms were filtered to cover the frequency range 60 Hz to 25 kHz in order to better highlight the sinusoidal nature of the waves. Since the response of the search coils is relatively flat in this part of the frequency calibration curve, we are able to present the magnetic component waveforms in nT, rather than in nT/sec as in Figure 1a. The data in Figure 2a were taken in the cusp TBL at 8.6 R_E, 12.5 MLT, and 62.3° λ_m. The magnetic channels show the presence of a sinusoidal waveform. Although not as obvious due to other activity, the electric components also show the presence of the sinusoidal waveform, as well as the presence of some higher frequency waves or turbulence, especially in the $E_{Z|}$ component. For example, just after 01:36:23.593 a pulse is observed that goes slightly positive before going to almost –0.4 mV/m and then back to about zero. Quasi-sinusoidal waveforms that appear as perturbations on top of the sinusoidal waveforms occur on much faster timescales than the pulse and are observed throughout the middle of the $E_{Z|}$ panel.

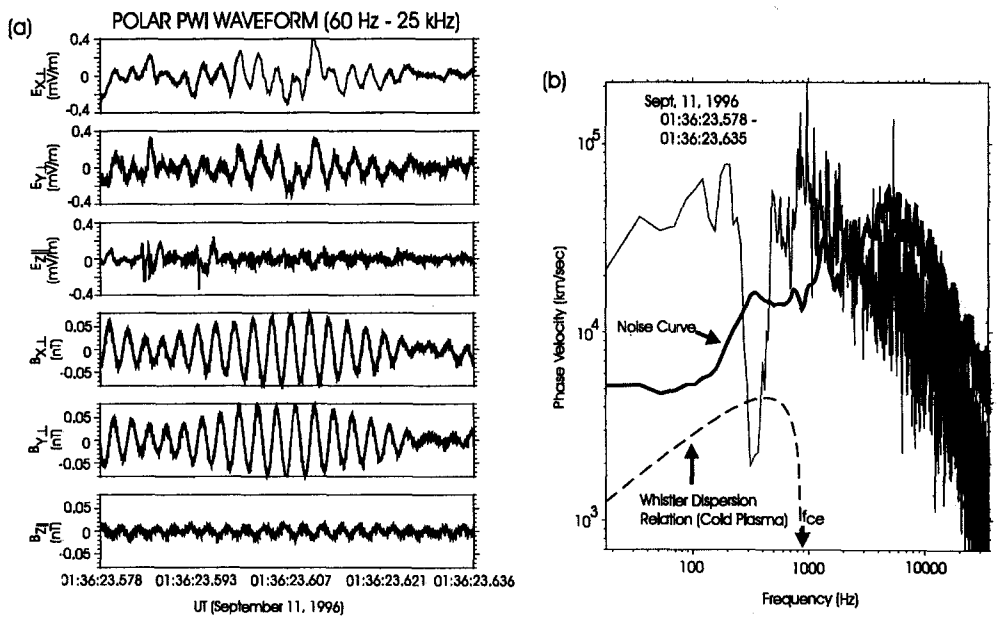

Fig. 2. (a) Recorded time series covering 57 ms from six channels of the Polar Plasma Wave Instrument transformed to a local magnetic field-aligned coordinate system. (b) Measured phase velocity (light solid line) obtained from the data plotted in (a), noise curve (solid dark line) determined from in-flight data with fluctuations above and below the noise curve indicating possible real emissions, and theoretical dispersion curve for Whistler Mode Waves (dashed line).

Transforming the full, unfiltered frequency range (20 Hz to 25 kHz) of the waveforms captured at the time shown in Figure 2a to the frequency domain, we obtain the spectrum shown in Figure 2b as the light solid line. Once again the solid dark line represents the noise curve obtained in the manner described above for the lower frequency waveforms. The coherent wave is now clearly seen extending well below the noise curve at around 350 Hz. In addition to this coherent wave, there appears to be turbulence at all frequencies from 60 Hz up to about 2 kHz. The turbulence is generally electrostatic but with a slight electromagnetic component up to f_{ce}. We speculate that the slightly increased electromagnetic nature is due to whistler mode turbulence. From f_{ce} up to about 1.5 kHz, we see the broad band associated with the pulses observed primarily in the waveform for E_{ZI}. From 1.5 kHz to about 8 kHz the turbulence observed in the spectrum is caused primarily by the electrostatic quasi-sinusoidal waveforms pointed out above. By quasi-sinusoidal we mean that the waveforms look nearly sinusoidal, but in fact the amplitude and period are constantly varying. As the frequency of these perturbations approaches 6-10 kHz, they appear to become more electromagnetic. This is not the case, however, as at these frequencies the quasi-sinusoidal waveforms are overlapping noise associated with the resonance of the search coils. Some of these quasi-sinusoidal waveforms, pulses and whistler mode waves are shown in higher time resolution in Figures 6 and 9 of Pickett et al. (2000) and in Figures 1 and 3 of Pickett et al. (1999a).

We have computed the cold plasma whistler dispersion relation curve, shown as the dashed line in Figure 2a, from the well-known analytical relation $v_w = c\{1+f_{pe}^2/[f(f_{ce}-f)]\}^{-1/2}$ where v_w is the phase velocity of the wave assuming propagation along the magnetic field, c is the speed of light, f_{pe} is the electron plasma frequency, f_{ce} is the electron cyclotron frequency, and f is the frequency of the wave. For the example shown in Figure 2b, the electron plasma frequency was about 29.1 kHz based on Polar Hydra electron data, and f_{ce} was about 870 Hz based on the measured magnetic field from Polar MFE. Here we see that the observed coherent wave at 350 Hz actually has a lower phase velocity than that given by whistler mode dispersion. We have determined that the coherent wave, which is right-hand polarized (obtained through minimum variance analysis), should be whistler mode based on the frequency range. See Pickett et al. (2000, 1999a) for more details on how this analysis is performed. The broadband electric component up to about 8 kHz is the result of performing an FFT on the pulse-like signatures and quasi-sinusoidal waveforms seen throughout the time series. Although this is not immediately apparent from Figure 2, the reader is referred to Pickett et al. (2000), where similar waveforms just after the time period shown here are analyzed in greater detail. An examination of the electric field waveform data in high time resolution shows that it is precisely the nonsinusoidal perturbations that are observed primarily along the E_{ZI} axis that are contributing to most of the electrostatic turbulence observed up to 8 kHz. This analysis is based on the characteristic period of each perturbation when transformed to the frequency domain by an FFT. Some of these perturbations come in packets that nearly resemble a sine wave with more than one period, hence the term quasi-sinusoidal, and others come as single pulses that are clearly evident in the waveforms.

Our last example is from a time period when the Polar spacecraft was reported to be in a region in which it skimmed along the magnetic separator and observed collisionless magnetic reconnection (Scudder, 2000), having just passed through the cusp TBL. Figure 3a shows the time series covering 0.5 s when the spacecraft was at 7.8 R_E, 12.0 MLT, and 72.9 λ_m. The data have been filtered to cover the frequency range 60 Hz to 2 kHz in order to better highlight the packetization of the magnetic waveforms. The noise curve in this figure varies quite dramatically from that of the overlapping range in Figure 2 primarily because it was difficult to find an extremely quiet region from which to create an in-flight noise floor for the 2 kHz filtered data. Further, because the 2 kHz filter is a digital filter (as opposed to the analog filter used in Figure 2), by its very nature it allows more low frequency noise to get through (in this case electrostatic noise). The 2 kHz bandpass filter used to obtain all of the data plotted in Figure 3b also falls off rapidly below 10 Hz, so the calibration is not valid below that frequency. Thus, the large spike observed around 8-9 Hz in the noise curve is real but falsely exaggerated since there is no way for us to adequately calibrate at that frequency. During the time period of Figure 3, f_{pe} was 45.3 kHz and f_{ce} was 1.5 kHz. Several waves are visible in Figure 3a, including more than one coherent electromagnetic wave, as well as several high frequency pulses and quasi-sinusoidal waveforms in the electric components primarily above f_{ce}, just as was seen in Figure 2. Since it is a well-known fact that the preamplifiers of the electric antennas on Polar oscillated throughout a larger time interval that includes the interval shown in Figure 3, we point out that they were definitely not oscillating during the precise interval shown in this figure. The oscillations produce significantly clipped waveforms in this receiver and such are not observed in Figure 3a.

The transformation to the frequency domain (Figure 3b) of the full, unfiltered frequency range (~2 Hz to 2 kHz) of the waveforms captured at the time shown in Figure 3a shows us that for this case, there are not only more than one whistler mode peaks, but there appears to be a general level of whistler mode turbulence (mixed whistler mode and electrostatic emission) in the frequency range from the lower hybrid up to nearly f_{ce}. Above that, we see a broad band that appears to be electrostatic in nature, just as we saw in Figure 2b, and which is associated with pulses and quasi-sinusoidal waveforms.

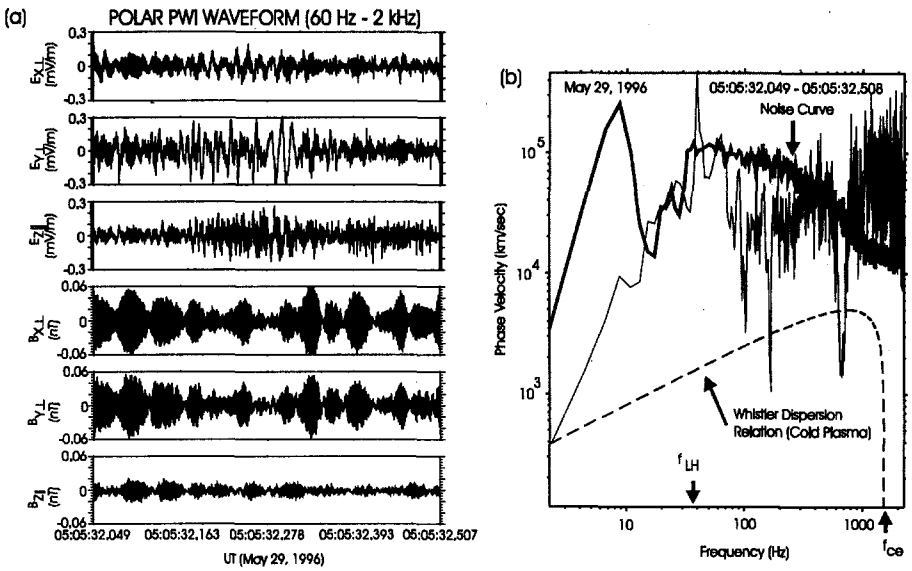

Fig. 3. (a) Recorded time series covering 459 ms. (b) Measured phase velocity, noise curve and theoretical dispersion curve for time series plotted in (a). Refer to Figure 2 caption for more information.

DISCUSSION AND SUMMARY

We have presented waveform observations made by the Polar spacecraft in and near the cusp Turbulent Boundary Layer at the magnetopause. We analyzed one case of low (1 Hz to 25 Hz) and two cases of high (<20 Hz up to 25 kHz) frequency observations of the phase velocity obtained from the measured wave electric to magnetic field ratio and compared these observations to the theoretical values obtained from the dispersion relations for kinetic Alfvén waves and whistler mode waves. We found that the low frequency electromagnetic turbulence observed below the lower hybrid frequency did not fit the KAW dispersion curve but tended toward it. The reason that the turbulence in this frequency range may not fit exactly on the KAW dispersion relation is probably related to the fact that during this period of time, the plasma beta was approximately 8-10. The theoretical KAW dispersion relation given above is applicable in the range less than 1 and greater than m_e/m_i. Thus, it would probably need to be modified to fit a plasma beta larger than 1. Based on the data showing a trend toward the KAW dispersion relation curve and the electric and magnetic components showing similar perturbations at the same times, we concluded that the turbulence was probably a mixture of modes, disbursive kinetic Alfvén waves and perhaps lower hybrid turbulence. This means that some of the turbulence in this frequency range may represent spatial turbulence of KAW that is Doppler-shifted to higher frequencies (in the spacecraft reference frame) by convective plasma flows (Stasiewicz et al., 2000a,b). The KAWs may act to energize ions and electrons and play a role in the transport of momentum and mass at the magnetopause layer (Stasiewicz et al., 2000b). Pickett et al. (2000) have suggested that the cusp turbulent boundary layer may be the exhaust region (or an extension thereof) of collisionless magnetic reconnection, according to the proposed theories of Mandt et al. (1994) and Drake (1995), that takes place closest to the site of reconnection. Their theories propose that scale lengths less than the ion inertial length are important in reconnection, and therefore whistler mode dynamics drive reconnection.

This leads us to the topic of the whistler mode waves and turbulence observed in the cusp TBL. The observed coherent whistler mode waves do not fit the cold plasma whistler mode dispersion relation, their values for phase velocity being lower than the theoretical ones. However, we assumed that these waves were propagating along the magnetic field with wave normal angles around 0°. The measured wave normal angles of the waves in the TBL usually fall in the range of 1-20°. Even if we account for this, the theoretical curve does not fit the measured values. One reason for this could be the error associated with the measurement of either f_{pe} or f_{ce}, which is used in obtaining the theoretical curve. Another possible reason could be that there is more than one plane wave present at any one frequency, perhaps propagating in different directions. More complex wave distribution function analysis is needed to determine this, which we are currently pursuing. Finally, and perhaps more importantly, is the possibility that the plasma is warm, requiring a modification to the cold plasma dispersion relation that we have used. Particle data for both cases presented in Figures 2 and 3 show that the plasma beta is around 1 to 10 and sometimes greater. With

regard to the electromagnetic turbulence observed in the frequency range between the lower hybrid resonance up to f_{ce}, it appears to be whistler mode mixed with electrostatic emission. Here we make the assumption that the electric and magnetic perturbations of the turbulence have the same proportionality as the waves from which the turbulence originates. One further consideration that has yet to be explored is the lower hybrid drift instability.

The electrostatic turbulence above f_{ce} has been shown in Pickett et al. (2000) and in the present work to be associated with pulses and quasi-sinusoidal waveforms observed in the time series. Ongoing work in this area should resolve the origin of these wave signatures. Pickett et al. (2000) have identified the pulses as potential structures, in this case electron holes based on earlier Polar research by Franz et al. (1998) and Mozer et al. (1997). For a full discussion of this topic, see Pickett et al. (2000) and references therein. Pickett et al. (2000) have also speculated that the quasi-sinusoidal waveforms observed in the electric field wave data may be a result of a modified two-stream instability. This instability is the resistive medium instability, which is characterized by a reduction in the electrostatic burst frequency below the electron plasma frequency, leading to the possibility that they are downshifted Langmuir waves. In the cusp TBL these particular waves appear to evolve (coalesce) into electron holes (Pickett et al., 2000), which would be in agreement with the theory of Goldman et al. (1999).

ACKNOWLEDGMENTS

We thank J. D. Scudder for the use of Polar Hydra data and C. T. Russell for the use of Polar MFE data in our study. We acknowledge support from NASA/Goddard Space Flight Center under Grant NAG5-7943.

REFERENCES

Drake, J. F., Magnetic Reconnection: A Kinetic Treatment, in Physics of the Magnetopause, eds. P. Song, B. U. Ö. Sonnerup, and M. F. Thomsen, Geophysical Monograph 90, pp. 155-165, American Geophysical Union, Washington, D.C., 1995.

Franz, J. R., P. M. Kintner, and J. S. Pickett, POLAR Observations of Coherent Electric Field Structures, *Geophys. Res. Lett.*, **25**, 1277-1280, 1998.

Goldman, M. V., M. M. Oppenheim, and D. L. Newman, Nonlinear Two-Stream Instabilities as an Explanation for Auroral Bipolar Wave Structures, *Geophys Res. Lett.*, **26**, 1821-1825, 1999.

Gurnett, D. A., A. M. Persoon, R. F. Randall, D. L. Odem, S. L. Remington, et al., The Polar Plasma Wave Instrument, *Space Sci. Rev.*, **71**, 597-622, 1995.

Mandt, M. E., R. E. Denton, and J. F. Drake, Transition to Whistler Mediated Magnetic Reconnection, *Geophys. Res. Lett.*, **21**, 73-76, 1994.

Mozer, F. S., R. Ergun, M. Temerin, C. Cattell, J. Dombeck, et al., New Features of Time Domain Electric-Field Structures in the Auroral Acceleration Region, *Phys. Rev. Lett.*, **79**, 1281-1284, 1997.

Pickett, J. S., D. A. Gurnett, J. D. Menietti, M. J. LeDocq, J. D. Scudder, et al., Plasma Waves Observed During Cusp Energetic Particle Events and Their Correlation with Polar and Akebono Satellite and Ground Data, *Adv. Space Res.*, **24**, 23-33, 1999a.

Pickett, J. S., J. D. Menietti, J. H. Dowell, D. A. Gurnett, and J. D. Scudder, Polar Spacecraft Observations of the Turbulent Outer Cusp/Magnetopause Boundary Layer of Earth, *Nonlin. Processes in Geophys.*, **6**, 195-204, 1999b.

Pickett, J. S., J. R. Franz, J. D. Scudder, J. D. Menietti, D. A. Gurnett, et al., Plasma Waves Observed in the Cusp Turbulent Boundary Layer: An Analysis of High Time Resolution Wave and Particle Measurements from the Polar Spacecraft, *J. Geophys. Res.*, in press, 2000.

Savin, S. P., N. L. Cordova, E. Yu. Budnik, A. O. Federov, S. I. Klimov, et al., Interball Tail Probe Measurements in Outer Cusp and Boundary Layers, in Geospace Mass and Energy Flow: Results from the International Solar-Terrestrial Physics Program, eds. J. L. Horwitz, D. L. Gallagher, and W. K. Peterson, Geophysical Monograph 104, 25-44, American Geophysical Union, Washington, D.C., 1998.

Scudder, J. D., Intersections on Magnetic Highways: A Sun Earth Connection, World Wide Web Link: http://www-st.physics.uiowa.edu/www/html/press_final/, 2000.

Stasiewicz, K., Y. Khotyanintsev, M. Berthomier, and J.-E. Wahlund, Identification of Widespread Turbulence of Dispersive Alfvén Waves, *Geophys. Res. Lett.*, **27**, 173-177, 2000a.

Stasiewicz, K., C. E. Seyler, F. S. Mozer, G. Gustafsson, J. Pickett, and B. Popielawska, Magnetic Bubbles and Kinetic Alfvén Waves in the High-Latitude Magnetopause Boundary, *J. Geophys. Res.*, submitted, 2000b.